ANTIOXIDANTS & REDOX SIGNALING
Volume 19, Number 14, 2013

DOI: 10.1089/ars.2012.5032

Therapeutics

ORIGINAL RESEARCH COMMUNICATION

A Low-Molecular-Weight Ferroxidase Is Increased in the CSF of sCJD Cases: CSF Ferroxidase and Transferrin as Diagnostic Biomarkers for sCJD

Swati Haldar,[1] 'Alim J. Beveridge,[2] Joseph Wong,[3] Ajay Singh,[1] Daniela Galimberti,[4] Barbara Borroni,[5] Xiongwei Zhu,[1] Janis Blevins,[1] Justin Greenlee,[6] George Perry,[7] Chinmay K. Mukhopadhyay,[8] Christine Schmotzer,[1] and Neena Singh[1]

Abstract

Aims: Most biomarkers used for the premortem diagnosis of sporadic Creutzfeldt-Jakob disease (CJD) are surrogate in nature, and provide suboptimal sensitivity and specificity. ***Results:*** We report that CJD-associated brain iron dyshomeostasis is reflected in the cerebrospinal fluid (CSF), providing disease-specific diagnostic biomarkers. Analysis of 290 premortem CSF samples from confirmed cases of CJD, Alzheimer's disease, and other dementias (DMs), and 52 non-DM (ND) controls revealed a significant difference in ferroxidase (Frx) activity and transferrin (Tf) levels in sporadic Creutzfeldt-Jakob disease (sCJD) relative to other DM and ND controls. A combination of CSF Frx and Tf discriminated sCJD from other DMs with a sensitivity of 86.8%, specificity of 92.5%, accuracy of 88.9%, and area-under-the receiver-operating-characteristic (ROC) curve of 0.94. This combination provided a similar diagnostic accuracy in discriminating CJD from rapidly progressing cases who died within 6 months of sample collection. Surprisingly, ceruloplasmin and amyloid precursor protein, the major brain Frxs, displayed minimal activity in the CSF. Most of the Frx activity was concentrated in the <3-kDa fraction in normal and diseased CSF, and resisted heat and proteinase-K treatment. ***Innovation:*** (i) A combination of CSF Frx and Tf provides disease-specific premortem diagnostic biomarkers for sCJD. (ii) A novel, nonenzymatic, nonprotein Frx predominates in human CSF that is distinct from the currently known CSF Frxs. ***Conclusion:*** The underlying cause of iron imbalance is distinct in sCJD relative to other DMs associated with the brain iron imbalance. Thus, change in the CSF levels of iron-management proteins can provide disease-specific biomarkers and insight into the cause of iron imbalance in neurodegenerative conditions. *Antioxid. Redox Signal*. 19, 1662–1675.

Introduction

RECENT YEARS HAVE SEEN a significant increase in the aging population and associated dementias (DMs). Intense efforts have therefore been directed at early diagnosis to enable initiation of available therapeutic strategies (33). Nevertheless, specific diagnosis is often missed or delayed until pathognomonic signs are obvious and neuronal death is irrevocable (67). An added concern is the misdiagnosis of potentially treatable DMs as sporadic Creutzfeldt-Jakob disease (sCJD), a uniformly fatal and potentially infectious DM with limited therapeutic options (10, 21, 29, 71, 72). Currently, definitive diagnosis of sCJD is established only after histopathological and biochemical analysis of brain tissue obtained by

Departments of [1]Pathology, [2]Organizational Behavior, and [3]Case Medical School, Case Western Reserve University, Cleveland, Ohio.
[4]Department of Pathophysiology and Transplantation, Centro Dino Ferrari, Fondazione Cà Granda, IRCCS Ospedale Maggiore Policlinico, University of Milan, Milan, Italy.
[5]Neurology Unit, Centre for Neurodegenerative Disorders, University of Brescia, Brescia, Italy.
[6]Virus and Prion Research Unit, National Animal Disease Center, ARS, USDA, Ames, Iowa.
[7]College of Sciences, The University of Texas at San Antonio, San Antonio, Texas.
[8]Special Centre for Molecular Medicine, Jawaharlal Nehru University, New Delhi, India.

Innovation

This study reports disease-specific biomarkers for the premortem diagnosis of Creutzfeldt-Jakob disease that are superior to the currently used surrogate biomarkers, and identifies a novel, nonenzymatic, nonprotein ferroxidase (Frx) in human cerebrospinal fluid (CSF). Contrary to the conventional belief, most of the Frx activity in human CSF is derived from a nonprotein, <3-kDa Frx rather than ceruloplasmin or amyloid precursor protein.

biopsy or at autopsy (1, 72). Available premortem diagnostic biomarkers are useful, but provide limited specificity, in distinguishing sCJD from other rapidly progressive DMs (21, 24, 25, 26, 27, 29, 35, 54, 68, 71). Retrospective studies by one center on the autopsy-confirmed cases of DM revealed incorrect classification of 32%–38% of rapidly progressive DMs as probable sCJD, almost half of which were later classified as Alzheimer's disease (AD), and others as frontotemporal DM (FTD), DM with Lewy bodies, progressive cerebral vasculitis (VS), infectious and paraneoplastic encephalitis (EN), and unclassified DM (10). Premortem diagnostic biomarkers of high sensitivity and specificity are therefore required for the accurate identification of sCJD (51).

Current diagnostic tests for sCJD include imaging techniques and identification of specific biomarkers in the cerebrospinal fluid (CSF) (31, 50, 75). Examination of CSF is widely used for the initial screening of DM, since it offers the advantage of low cost, ease of performance, and reasonable accuracy. The World Health Organization (WHO) criteria for probable diagnosis of sCJD require positive identification of 14-3-3 in the CSF and a typical electroencephalogram pattern (74). However, most diagnostic centers use a combination of CSF biomarkers and imaging to achieve a higher degree of sensitivity and specificity. A combination of fluid-attenuated inversion recovery, diffusion-weighed magnetic resonance imaging, and WHO-proposed criteria provide a sensitivity of 98% and specificity of 70.8% in discriminating sCJD from other DMs (75). CSF levels of 14-3-3 and total-tau (t-tau), lactate dehydrogenase, S100B, neuron-specific enolase (NSE), and several other biomarkers used singly or in different combinations provide variable sensitivity and specificity, depending on the patient population tested, cutoff used for diagnosis, and experimental protocol. A review of the literature from 1995 to 2011 on the accuracy of 14-3-3 as a diagnostic test for sCJD revealed a sensitivity of 92% and specificity of 80% (46). A 6-year prospective study on clinically suspected cases of sCJD from Canada indicated a sensitivity and specificity of 88% and 72% for 14-3-3, 91% and 88% for tau, and 87% for S100B (15). A 10-year study from the National CJD Surveillance Center in the United Kingdom reported a sensitivity of 86% and specificity of 74% for 14-3-3, 81% and 84% for tau, and 65% and 90% for S100B. A combination of all three biomarkers increased the specificity to 96%, but decreased the sensitivity considerably to 57% (12). A similar study in the United States reported a sensitivity and specificity of 90% and 40% for 14-3-3, and 87% and 67% for tau (30, 53).

A probable reason for suboptimal accuracy of the above biomarkers is their association with other neurodegenerative conditions in addition to sCJD. Thus, 14-3-3, NSE, and S100B are elevated up to 100-fold in aneurysmal subarachnoid hemorrhage, and to variable degrees in other neurodegenerative conditions (27, 57). Likewise, tau is elevated in AD and other DMs, decreasing its diagnostic specificity (56). Disease-specific biomarkers for sCJD are limited, and include a change in the levels of normal prion protein (PrP^{C}) (70) and identification of protease-resistant PrP-scrapie (PrP^{Sc}) in the CSF (49). When used as diagnostic biomarkers, measurement of CSF levels of PrP^{C} provides a sensitivity of 76% and specificity of 88%, and PrP^{Sc} amplified by real-time quaking-induced conversion reveals a sensitivity of 80% and specificity of 100% (2, 70). Although related to the underlying pathology, these biomarkers fall short of the desired expectations, since the levels of PrP^{C} are altered in other neurodegenerative conditions besides sCJD, and spontaneous conversion of PrP^{C} to PrP^{Sc} has been reported in some instances by the real-time quaking technique (14, 43).

Recent reports indicate imbalance of brain iron homeostasis as a common feature of certain neurodegenerative disorders, in particular sCJD, AD, Parkinson's disease (PD), and Huntington's disease (HD) (3, 6, 8, 19, 34, 37, 60, 64, 65, 73). The underlying cause of iron imbalance is distinct in each case, and partly stems from the involvement of key proteins responsible for the pathogenesis of these disorders in cellular iron metabolism (17, 22, 32, 61, 62). Since homeostasis of iron is maintained by the coordinated effort of iron uptake, storage, and efflux proteins, altered function of one is expected to cause a distinct change in others, some of which are reflected in the CSF (59).

To explore this possibility, the levels of ferritin, soluble transferrin (Tf) receptor, Tf, ceruloplasmin (Cp), amyloid precursor protein (APP), and ferroxidase (Frx) and ferrireductase activities were checked in premortem CSF from cases of sCJD ($n=98$), AD ($n=62$), FTD ($n=31$), DM of vascular origin (VS) ($n=13$), EN ($n=13$), non-CJD DMs (other-DMs) ($n=73$), and age-matched non-DM (ND) controls ($n=52$) (Supplementary Table S1A–D; Supplementary Data are available online at www.liebertpub.com/ars). We describe the accuracy of different biomarkers in discriminating sCJD from AD, other-DM, all DMs grouped together (all-DM), and ND controls when used individually or in different combinations. Biomarkers with best performance were checked for their accuracy in discriminating sCJD from the DM cases who died within 6 months of sample collection, and were considered rapidly progressive for the purposes of this study. We also describe a novel Frx in human CSF that is distinct from the currently known brain Frxs, Cp and APP (22, 28, 36).

Results

A total of 342 premortem samples of CSF from four centers were tested (Supplementary Table S1A–D). Diagnosis of all CJD and 73 other-DM cases was confirmed by autopsy. For others, probable diagnosis was provided based on clinical and laboratory tests. The duration between sample collection and time of death was <6 months for 80 CJD, 18 AD, 13 VS, 13 EN, and 60 other-DM cases. For most ND and DM cases, total protein, red and white cell count, and glucose levels were known. Aliquots of all samples were flash-frozen at −80°C immediately after collection and discarded after one thaw.

Frx activity is increased in the CSF of sCJD cases

A recent report demonstrated reduced Frx activity of APP in the AD brains and consequent accumulation of iron in affected neurons (22). To evaluate whether this change is reflected in the CSF and differs from brain iron imbalance in

CJD and other DMs, Frx activity in the CSF was compared across disease groups. Accordingly, oxidation of freshly prepared ferrous ammonium sulfate (FAS) (Fe^{2+}) by a fixed volume of CSF was quantified by measuring the change in color of apo-Tf (22) or ammonium thiocyanate on binding to Fe^{3+} ions (4, 5). Both methods yielded similar results (Fig. 1A–D) (Supplementary Fig. S1). Data from the ammonium thiocyanate procedure are shown in this report. For all measurements, two samples from the ND group were included as an internal standard. Negative controls included reaction mixes lacking CSF or FAS. The latter was included to rule-out artifactual release of iron from CSF Tf. Purified Cp was included as a positive control. Frx activity was quantified based on a standard curve established from graded concentrations of FAS and purified Cp over a time course. Triplicates of each CSF sample were tested, and the experiment was repeated a minimum of three times.

Comparison of sCJD ($n = 94$) relative to the ND ($n = 52$) and all-DM ($n = 192$) samples revealed significantly higher Frx

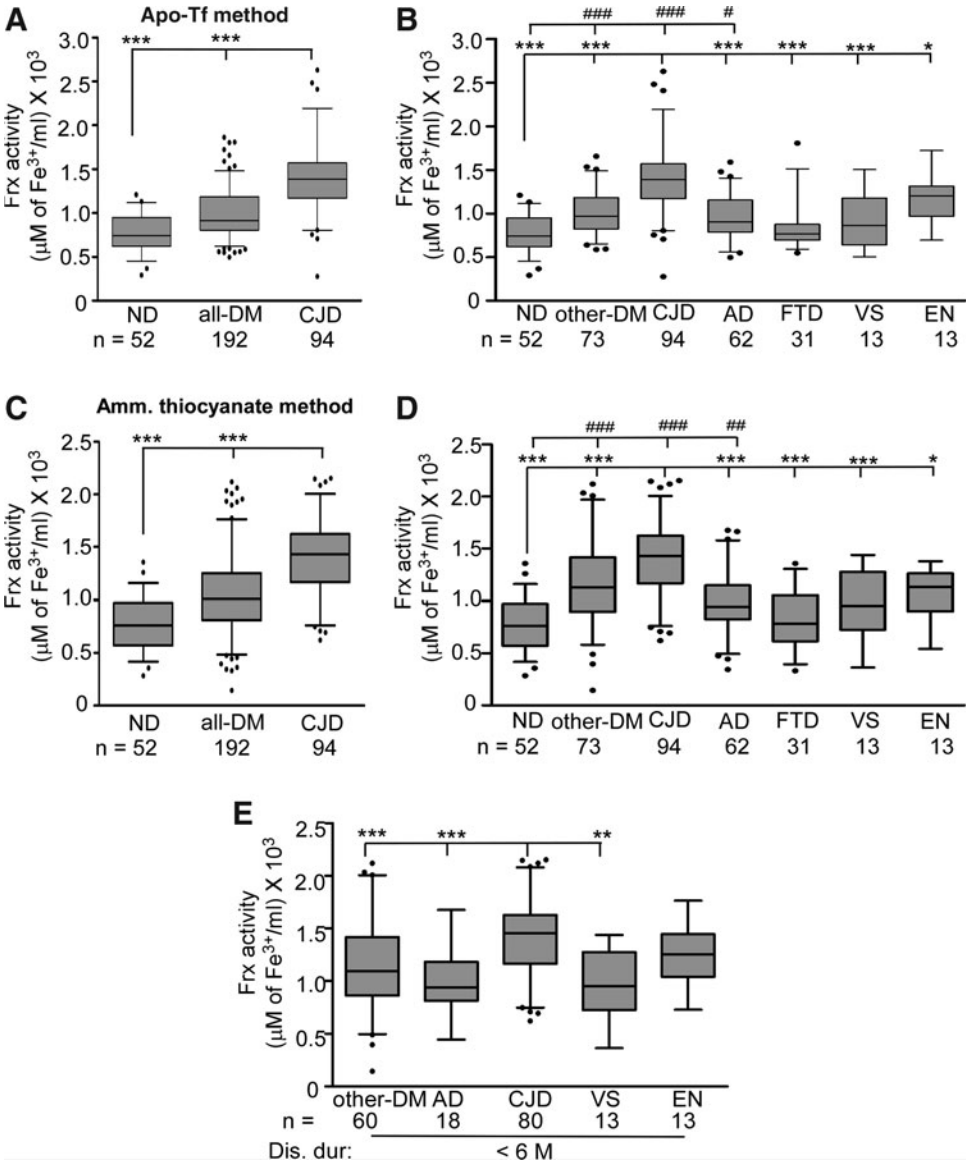

FIG. 1. Frx activity is increased in CJD relative to the all-DM and ND samples. Box-and-whisker plots of CSF Frx activity measured by the apo-Tf method (22) **(A, B)** and ammonium thiocyanate method (5) **(C, D)** with median, 25–75th percentiles, and outliers. The top and bottom of the box represent 75 and 25th percentile, respectively, while the whiskers represent the highest and lowest values. Values over 1.5 times the interquartile range have been treated as outliers and are shown as closed circles away from the whiskers. Significance of differences was calculated by ANOVA. **(A, C)** Frx activity in CJD samples is significantly higher than the all-DM and ND samples. $^{***}p < 0.001$. **(B, D)** Frx activity in CJD samples is significantly higher than other-DM, ND, AD, FTD, VS, and EN samples. $^{***}p < 0.001$; $^{**}p < 0.01$; $^{*}p < 0.05$. Frx activity of ND samples is significantly lower than other-DM, CJD, and AD cases. $^{###}p < 0.001$; $^{##}p < 0.01$; $^{#}p < 0.05$. **(E)** Frx activity in CJD samples with a disease duration of < 6 *M* (time between sample collection and death) is significantly higher than other-DM, AD, and VS samples. $^{***}p < 0.001$; $^{**}p < 0.01$. AD, Alzheimer's disease. CSF, cerebrospinal fluid; CJD, Creutzfeldt-Jakob disease; DM, dementia; EN, encephalitis; Frx, ferroxidase; FTD, frontotemporal dementia; ND, nondementia; VS, progressive cerebral vasculitis.

activity in sCJD relative to the ND and all-DM samples (Fig. 1A, C). A similar difference was noted between sCJD relative to AD, FTD, VS, EN, other-DM, and ND samples (Fig. 1B, D). However, when compared with ND, only other-DM, sCJD, and AD samples showed a significant difference. Frx activity in FTD, VS, and EN samples differed minimally from ND cases (Fig. 1B, D).

To determine if Frx activity is influenced by the rapidity of disease progression, cases who died within 6 months of sample collection were tested. Samples for which this information was not available were excluded from the analysis. As noted above, Frx activity was significantly higher in sCJD relative to AD, other-DM, and VS samples. The difference between the sCJD and EN cases was insignificant in this group (Fig. 1C). There was no influence of age at the time of sample collection on Frx activity or t-Tf levels (see below) (Supplementary Fig. S2A, B).

Frx activity in the CSF does not correspond to Cp or APP levels

To identify the source of increased Frx activity in CJD samples, levels of the major brain Frxs Cp and APP were estimated (22). Since albumin is the major protein in CSF and varies significantly in different disease conditions, equal volume of CSF rather than equal protein from CJD and all-DM samples was subjected to Western blotting and reacted with Cp- and APP-specific antibodies. No apparent differences in the Cp levels were observed between these groups in a representative blot (Fig. 2A) and by densitometric analysis (Fig. 2B) despite significant differences in total protein content (Supplementary Table S1). In contrast, the same samples showed significantly higher Frx activity in sCJD relative to all-DM samples (Fig. 2C). A similar evaluation of APP showed a significant increase in other-DM samples relative to the ND and sCJD samples (Fig. 2D). The difference between other groups was not significant (Fig. 2D). Thus, increased Frx activity in sCJD samples is not due to a corresponding increase in the Cp or APP levels.

To evaluate significant differences in other proteins involved in the brain iron metabolism, levels of Tf, soluble Tf receptor, and ferritin were checked. Western blotting followed by densitometry showed a significant decrease in total Tf (Tf-1 + Tf-β2) in sCJD relative to ND, other-DM, AD, and EN cases (Fig. 2E). A representative blot of the all-DM and

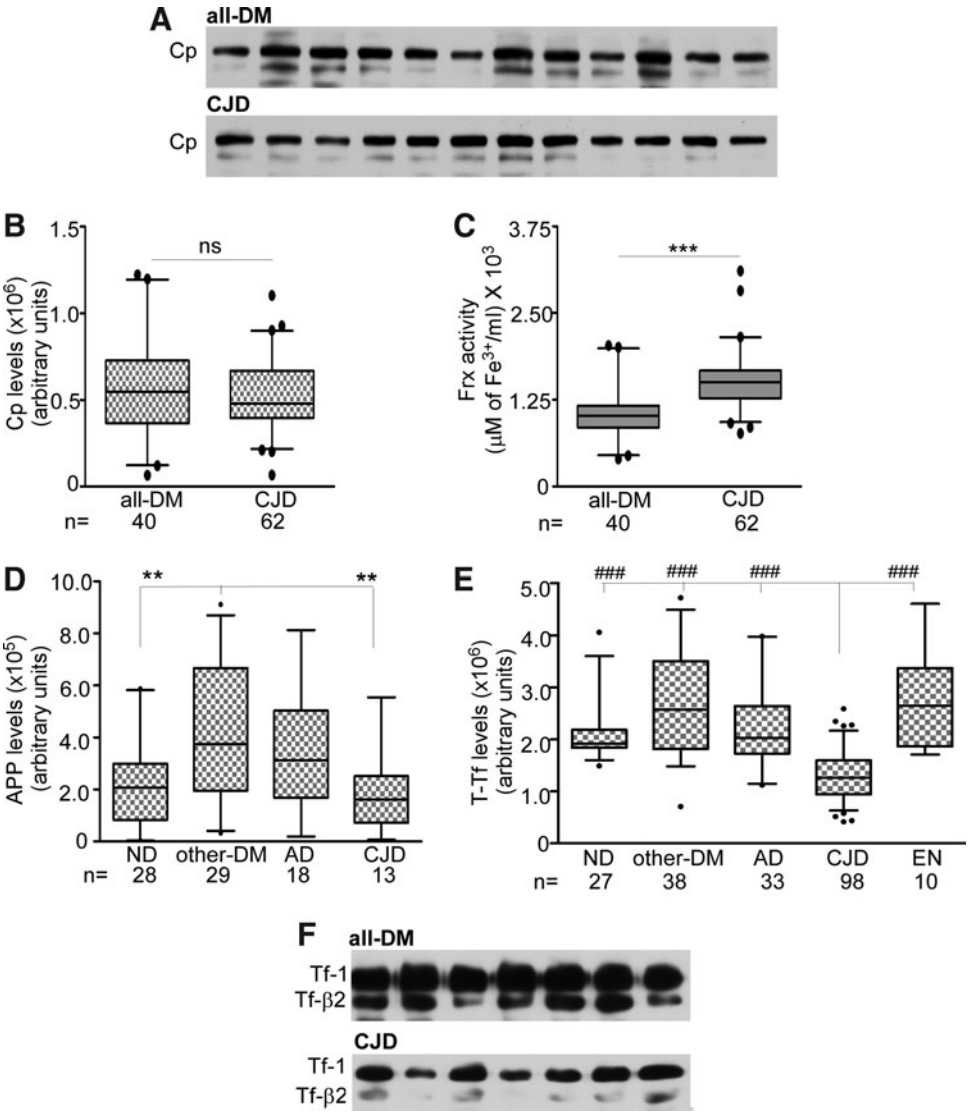

FIG. 2. Cp is not the major Frx in human CSF. (A) Representative immunoblots showing no change in Cp levels between the all-DM and CJD samples. **(B)** Box-and-whisker plots representing quantification of the Cp levels by densitometry. The difference between the all-DM and CJD samples is not significant. **(C)** Frx activity in samples from **(A)** is significantly more in CJD relative to all-DM samples. $^{***}p < 0.001$. **(D)** Quantification of APP by immunoblotting followed by densitometry shows significantly higher levels in other-DM relative to ND and CJD samples. $^{**}p < 0.01$. **(E)** Quantification of Tf expression shows significantly lower levels in CJD relative to the ND, other-DM, AD, and EN samples. $^{\#\#\#}p < 0.001$. **(F)** Representative immunoblot of CSF Tf from all-DM and CJD samples. APP, amyloid precursor protein; Cp, ceruloplasmin; Tf, transferrin.

Table 1. Performance of Single Biomarkers in Discriminating Sporadic Creutzfeldt-Jakob Disease from All Dementias, Including Alzheimer's Disease, and from Alzheimer's Disease and Frontotemporal Dementia Separately

	CJD vs. *DM (all)*			*CJD* vs. *AD*			*CJD* vs. *FTD*
Biomarker	*Frx*	*t-Tf*	*t-tau*	*Frx*	*t-Tf*	*t-tau*	*Frx*
n	CJD (94) DM (167)	CJD (98) DM (71)	CJD (95) DM (90)	CJD (94) AD (62)	CJD (98) AD (33)	CJD (95) AD (25)	CJD (94) FTD (31)
T-test							
t statistic	−7.61	9.75	−6.43	−7.75	6.37	−7.93	−7.03
p-Value	<0.001	<0.001	<0.001	<0.001	<0.001	<0.001	<0.001
Area under ROC (95% CI)	0.77 (0.71–0.83)	0.89 (0.84–0.94)	0.84 (0.78–0.90)	0.82 (0.75–0.88)	0.86 (0.80–0.93)	0.90 (0.83–0.97)	0.88 (0.80–0.95)
Sensitivity (95% CI)	85.1 (75.9–91.3)	84.7 (75.7–90.9)	86.3 (77.4–92.2)	85.1 (75.9–91.3)	92.9 (85.3–96.8)	86.3 (77.4–92.2)	85.1 (75.9–91.3)
Specificity (95% CI)	52.7 (44.9–60.4)	70.4 (58.2–80.4)	73.3 (62.8–81.9)	61.3 (48.0–73.1)	63.6 (45.1–79.0)	84.0 (63.1–94.7)	71.0 (51.8–85.1)
Positive LR (95% CI)	1.8 (1.5–2.2)	2.9 (2.0–4.1)	3.2 (2.3–4.6)	2.2 (1.6–3.0)	2.6 (1.6–4.0)	5.4 (2.2–13.3)	2.9 (1.7–5.1)
Negative LR (95% CI)	0.3 (0.2–0.5)	0.2 (0.1–0.4)	0.2 (0.1–0.3)	0.2 (0.1–0.4)	0.1 (0.1–0.2)	0.2 (0.1–0.3)	0.2 (0.1–0.4)
PPV (%) (95% CI)	50.3 (42.3–58.3)	79.8 (70.6–86.8)	77.4 (68.0–84.7)	76.9 (67.4–84.4)	88.3 (80.2–93.6)	95.3 (87.9–98.5)	89.9 (81.2–95.0)
NPV (%) (95% CI)	86.3 (77.7–92.0)	76.9 (64.5–86.1)	83.5 (73.1–90.6)	73.1 (58.7–84.0)	75.0 (54.8–88.6)	61.8 (43.6–77.3)	61.1 (43.5–76.4)
Accuracy	64.4	78.7	80.0	75.6	85.5	85.8	81.6

Variability in sample numbers is due to insufficient sample volume for quantifying some biomarkers.
AD, Alzheimer's disease; DM, dementia; FTD, frontotemporal dementia; NPV, negative predictive value; PPV, positive predictive value; Tf, transferrin; LR, likelihood ratios.

CJD samples is shown (Fig. 2F). Other proteins showed a minimal difference between the disease groups (data not shown).

Together, these observations show that Frx activity is increased, and Tf is decreased in the CSF from sCJD cases, and these changes are not influenced by age, end-stage disease, or rapid disease progression. More importantly, there is no correlation between CSF Frx activity and Cp or APP levels, suggesting the presence of an alternate Frx in human CSF. Subsequent investigations were focused on the usefulness of CSF Frx and Tf as premortem diagnostic biomarkers of sCJD, and identifying the source of Frx activity in the CSF.

Accuracy of CSF Frx and Tf as diagnostic biomarkers of sCJD

Since 14-3-3 and t-tau are used routinely for the diagnosis of CJD, levels of these proteins were quantified by Western blotting and ELISA, respectively (Supplementary Table S1 and Tables 1–4). Using logistic regression (described below), 14-3-3 revealed a sensitivity of 93.7%, but a very poor specificity of 21.1% in discriminating CJD from all-DM cases. When combined with t-tau, the specificity improved to 50% with only a slight drop in sensitivity to 91.3% (Supplementary Table S2.

Next, the performance of Frx, t-Tf, and t-tau as diagnostic biomarkers of CJD was compared. *T*-test results indicated highly significant differences between CJD relative to the all-DM, AD, and FTD cases for all three biomarkers (Table 1). When used individually, the specificity of Frx, t-Tf, and t-tau in discriminating CJD from all-DM was 52.7%, 70.4%, and 73.3%, and from AD 61.3%, 63.6%, and 84.0%, respectively. Frx activity discriminated CJD from FTD with a specificity of 71.0% (Table 1) (t-Tf and t-tau were not tested for FTD cases because of limited sample volume). Next, samples from a single center with complete biomarker data were tested to rule out bias due to collection and storage (Table 2). When used singly, biomarker performance was similar to the values in Table 1 as expected. However, a combination of Frx and t-Tf discriminated CJD from all-DM and AD with an improved specificity of 92.5% (Table 2) and 93.3% (Table 3). Addition of t-tau to the Frx and t-Tf combination increased the sensitivity of CJD diagnosis relative to all-DM from 86.8% to 90.1%, but decreased the specificity from 92.5% to 90.6% (Table 2). The t-tau, Frx, and t-Tf combination did not increase the sensitivity or specificity of discrimination between sCJD and AD significantly (Table 3). The performance of all single biomarkers improved when combined with other biomarkers, but none of the combinations exceeded the accuracy of the Frx and t-Tf combination in discriminating sCJD from all-DM or AD (Tables 2 and 3).

Other diagnostic parameters such as area under the curve (AUC), positive likelihood ratios (LR), negative LR, positive predictive value (PPV), negative predictive value (NPV), Aikake-Information-Criterion (AIC), and accuracy improved upon combining Frx and Tf (Table 2). Addition of t-tau to this combination improved the sensitivity and specificity above 90% and AUC of 0.95. Consequentially, the predictive accuracy also increased to more than 90%. A lower AIC of 0.57 made this model promising. However, a comparison of the Frx and t-Tf combination with the triple biomarker combination showed that the addition of t-tau did not provide significant gains, as the difference in the AUC was insignificant ($p = 0.11$). In addition to comparable specifications with the triple biomarker combination (0.94 AUC, 86.8% sensitivity, 92.5% specificity, 88.9% accuracy, and a low AIC of 0.67) (Table 2), the Frx and t-Tf combination was more parsimonious. In contrast, Frx combined with T-tau yielded a

Table 2. Performance of Single and Biomarker Combinations in Discriminating Sporadic Creutzfeldt-Jakob Disease from All Dementias, Including Alzheimer's Disease

	Single biomarkers			*Biomarkers combinations*			
Biomarker	*Frx*	*t-Tf*	*t-tau*	*Frx & t-Tf*	*Frx & t-tau*	*t-Tf & t-tau*	*Frx & t-Tf & t-tau*
Area under ROC (95% CI)	0.75 (0.67–0.84)	0.89 (0.84–0.95)	0.82 (0.74–0.90)	0.94 (0.89–0.98)	0.83 (0.75–0.90)	0.93 (0.88–0.97)	0.95 (0.92–0.99)
Sensitivity (95% CI)	85.7 (76.4–91.9)	87.9 (79–93.5)	87.9 (79–93.5)	86.8 (77.7–92.7)	85.7 (76.4–91.9)	85.7 (76.4–91.9)	90.1 (81.6–95.1)
Specificity (95% CI)	49.1 (35.3–63)	71.7 (57.4–82.8)	69.8 (55.5–81.3)	92.5 (80.9–97.6)	66.0 (51.6–78.1)	83.0 (69.7–91.5)	90.6 (78.6–96.5)
Positive LR (95% CI)	1.7 (1.3–2.2)	3.1 (2–4.8)	2.9 (1.9–4.4)	11.5 (4.5–29.6)	2.5 (1.7–3.7)	5 (2.8–9.2)	9.6 (4.1–22.1)
Negative LR (95% CI)	0.3 (0.2–0.5)	0.2 (0.1–0.3)	0.2 (0.1–0.3)	0.1 (0.1–0.2)	0.2 (0.1–0.4)	0.2 (0.1–0.3)	0.1 (0.1–0.2)
PPV (%) (95% CI)	74.30 (64.7–82.1)	84.2 (75–90.6)	83.3 (74–89.9)	95.2 (87.5–98.4)	81.3 (71.7–88.2)	89.7 (80.8–94.9)	94.3 (86.5–97.9)
NPV (%) (95% CI)	66.70 (49.7–80.4)	77.60 (63–87.8)	77.1 (62.3–87.5)	80.3 (67.8–89)	72.90 (57.9–84.3)	77.20 (63.8–86.8)	84.2 (71.6–92.1)
AIC	1.16	0.79	1.18	0.62	1.07	0.68	0.57
Accuracy	72.2	81.9	81.3	88.9	78.5	84.7	90.3

CJD ($n=91$) *vs.* DM ($n=53$).
Samples with all three biomarker values were used for this analysis.

significantly lower AUC (0.83) than the Frx and t-Tf combination ($p<0.01$) and showed low specificity (66%), low accuracy (78.5%), and high AIC (1.07), and therefore did not fit the specifications of a good predictive model. t-tau combined with t-Tf had high accuracy (84.7%), low AIC (0.68), but a significantly lower AUC (0.93), than the triple biomarker combination ($p=0.03$) and comparatively low specificity (83%). Therefore, the new biomarker combination of Frx and t-Tf showed better performance in discriminating sCJD from all-DM, as is also obvious from its highest positive LR (11.5).

An equally promising performance of the Frx and t-Tf combination was noted in discriminating sCJD from rapidly progressive cases, revealing a sensitivity of 88.6%, specificity of 91.8%, PPV of 94.6%, NPV of 83.3%, accuracy of 89.8%, and AUC of 0.94 (Table 4).

The accuracy of the Frx and t-Tf combination as a diagnostic test is shown graphically by the ROC curve, which depicts the tradeoff between sensitivity and specificity for all possible cutoff values (Fig. 3A). Area-under-the-ROC curve for this combination was 0.94, which is greater than or equal to the AUC for other biomarkers when used individually or in combination (Tables 1–4). The discriminative power of Frx (y) and t-Tf (x) as a potential diagnostic test for sCJD was checked further by deriving an equation based on logistic regression analysis at a sensitivity of ~85% (41), and plotted as a straight line in the scatter graph of CJD, AD, FTD, and other-DM cases (excluding AD and FTD) (Fig. 3B). There was little overlap between the disease groups. Thus, the Frx and t-Tf combination discriminates sCJD from all-DM, AD, and rapidly progressive cases with a superior discriminative power, that is,

Table 3. Performance of Single and Biomarker Combinations in Discriminating Sporadic Creutzfeldt-Jakob Disease from Alzheimer's Disease

	Single biomarkers			*Biomarkers combinations*			
Biomarker	*Frx*	*t-Tf*	*t-tau*	*Frx & t-Tf*	*Frx & t-t-tau*	*t-Tf & t-tau*	*Frx, t-Tf & t-tau*
Area under ROC (95% CI)	0.78 (0.66–0.91)	0.87 (0.77–0.97)	0.91 (0.82–1.00)	0.94 (0.88–1.00)	0.92 (0.84–1.00)	0.94 (0.89–1.00)	0.98 (0.95–1.00)
Sensitivity (95% CI)	85.7 (76.4–91.9)	93.4 (85.7–97.3)	85.7 (76.4–91.9)	85.7 (76.4–91.9)	85.7 (76.4–91.9)	89 (80.3–94.3)	86.8 (77.7–92.7)
Specificity (95% CI)	60.0 (32.9–82.5)	66.7 (38.7–87.0)	86.7 (58.4–97.7)	93.3 (66.0–99.7)	86.7 (58.4–97.7)	86.7 (58.4–97.7)	93.3 (66–99.7)
Positive LR (95% CI)	2.1 (1.1–4)	2.8 (1.4–5.7)	6.4 (1.8–23.4)	12.9 (1.9–85.6)	6.4 (1.8–23.4)	6.7 (1.8–24.3)	13.0 (2.0–86.6)
Negative LR (95% CI)	0.2 (0.1–0.5)	0.1 (0.0–0.2)	0.2 (0.1–0.3)	0.2 (0.1–0.3)	0.2 (0.1–0.3)	0.1 (0.1–0.2)	0.1 (0.1–0.2)
PPV (%) (95% CI)	92.9 (84.5–97.1)	94.4 (86.9–97.9)	97.5 (90.4–99.6)	98.7 (92.2–99.9)	97.5 (90.4–99.6)	97.6 (90.8–99.6)	98.8 (92.3–99.9)
NPV (%) (95% CI)	40.9 (21.5–63.3)	62.5 (35.9–83.7)	50.0 (30.4–69.6)	51.9 (32.4–70.8)	50.0 (30.4–69.6)	56.5 (34.9–76.1)	53.8 (33.7–72.9)
AIC	0.72	0.59	0.61	0.42	0.53	0.44	0.35
Accuracy	82.1	89.6	85.8	86.8	85.8	88.7	87.7

CJD ($n=91$) *vs.* AD ($n=15$).
Samples with all three biomarker values were used for this analysis.
CI, confidence interval.

Table 4. Performance of Single and Biomarker Combinations in Discriminating Sporadic Creutzfeldt-Jakob Disease from Rapidly Progressive Dementia, Including Alzheimer's Disease

Biomarker	*Frx*	*Frx & t-Tf*	*Ferrox, t-Tf & t-tau*
Area under ROC (95%CI)	0.76 (0.67–0.85)	0.94 (0.89–0.99)	0.96 (0.92–0.99)
Sensitivity (95%CI)	86.1 (76–92.5)	88.6 (79–94.3)	91.1 (82–96.1)
Specificity (95%CI)	51.0 (36.5–65.4)	91.8 (79.5–97.4)	89.8 (77–96.2)
Positive LR (95%CI)	1.8 (1.3–2.4)	10.9 (4.2–27.9)	8.9 (3.9–20.6)
Negative LR (95%CI)	0.3 (0.1–0.5)	0.1 (0.1–0.2)	0.1 (0–0.2)
PPV (%) (95%CI)	73.9 (63.5–82.3)	94.6 (86–98.3)	93.5 (84.8–97.6)
NPV (%) (95%CI)	69.4 (51.7–83.1)	83.3 (70.2–91.6)	86.3 (73.1–93.8)
Accuracy	72.7	89.8	90.6

Disease duration <6 months.
CJD ($n=79$) *vs.* DM ($n=49$).
Samples with all three biomarker values were used for this analysis.

sensitivity 86.8%, specificity 92.5%, ROC 0.94, PPV 95.2, NPV 80.3, and accuracy 88.9 (Tables 1–4), than the currently used CSF biomarkers (12, 30, 31, 46, 53).

CSF Frx is distinct from Cp and APP

To determine the source of increased Frx activity in CJD samples, CSF was fractionated based on the molecular mass to evaluate the contribution of Cp, APP, and other uncharacterized Frxs to this activity. For initial standardization, CSF samples from the ND cases were fractionated concomitantly through filter membranes with molecular-mass cutoff of 100, 50, or 3 kDa, and Frx activity of each fraction was tested. Unfractionated CSF (whole) and appropriately diluted purified Cp were analyzed in parallel (Fig. 4A). As expected, Frx activity from Cp was detected in >100-, >50-, and >3-kDa fractions. Surprisingly, almost all Frx activity in the CSF was recovered in the <3-kDa fraction (Fig. 4A).

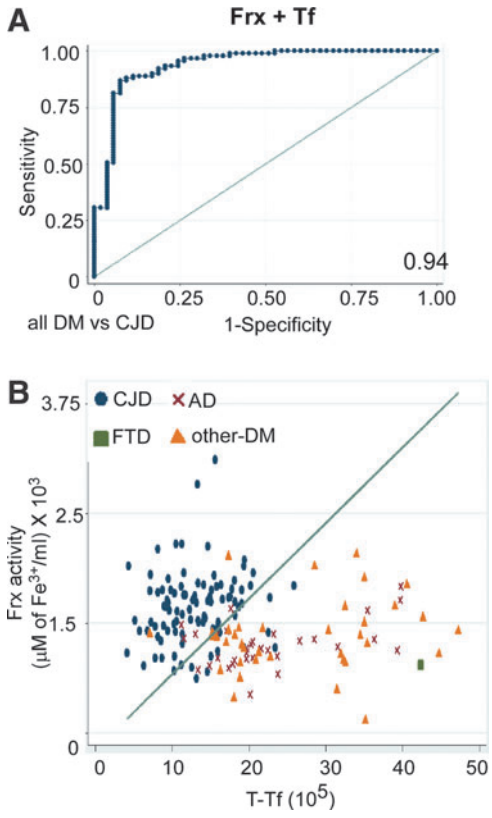

FIG. 3. CSF Frx and Tf as a diagnostic test for CJD. (A) The ROC curve of CSF Frx activity in combination with Tf. The area under the ROC is 0.94. **(B)** Scatter graph showing separation of CJD cases from AD, FTD, and other DMs. Reference line shows cutoff equation derived to achieve a sensitivity of ~85%. To see this illustration in color, the reader is referred to the web version of this article at www.liebertpub.com/ars

Next, an additional sample was included where purified Cp was mixed with CSF. Samples were either set aside (whole) or fractionated through 50-kDa filters. The resultant filtrate was passed through 3-kDa filters to obtain fractions >50 kDa, between 50 and 3 kDa, and <3 kDa (Fig. 4B). Frx activity in an unfractionated (whole) sample represents the sum total of Cp and CSF Frx activity individually. When passed through the 50-kDa filter, samples containing Cp (Cp) and Cp added to CSF (CSF+Cp) retain their activity in the >50-kDa fraction, while CSF shows no activity in this fraction. In fact, the activity of CSF+Cp samples falls to the levels equivalent to purified Cp in this fraction. Subsequent fractionation reveals almost all Frx activity from CSF in the <3-kDa fraction, indicating that while activity from Cp is detected in the >50-kDa fraction, almost all of the activity from the CSF is concentrated in the <3-kDa fraction (Fig. 4B).

Subsequently, the unfractionated Cp, Cp+CSF, and CSF samples were treated with proteinase-K (PK) to eliminate most of the proteins, and residual Frx activity was compared with untreated controls. As expected, PK destroyed Frx activity of purified Cp completely, and caused a significant reduction in the Cp+CSF samples. Surprisingly, PK had no effect on CSF Frx activity (Fig. 4C).

Fractionation of the DM and sCJD samples with purified Cp as a positive control revealed 1.5-fold more Frx activity in sCJD relative to the age-matched DM samples as in Figure 1 above. Again, almost all Frx activity in DM and sCJD samples was restricted to the <3-kDa fraction (Fig. 4D). A similar evaluation of human serum from healthy donors revealed most of the Frx activity in the >100-kDa fraction, consistent with Cp as the major serum Frx (data not shown).

Absence of Frx activity in the >100-kDa fraction of CSF where majority of Cp and APP are expected to partition was surprising. We therefore concentrated CSF proteins 10-fold by methanol precipitation before estimating Frx activity. Mouse brain homogenates that display significant Cp- and APP-

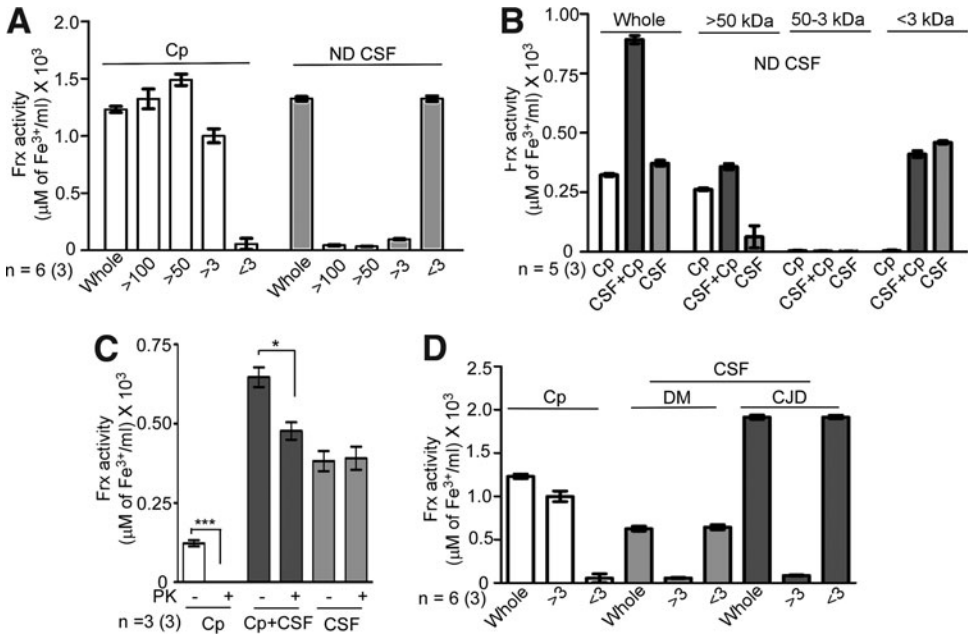

FIG. 4. CSF Frx activity is concentrated in the <3-kDa fraction. (A) CSF from ND cases was fractionated through the filters with different molecular-mass cutoffs. Unfractionated CSF (whole) and purified Cp were processed in parallel. Almost all Frx activity of Cp is detected in the retentate of the 100-kDa, 50-kDa, and 3-kDa filters (>100, >50, and >3) as expected. In contrast, most of the activity from CSF is detected in the <3-kDa filtrate (<3). Data are means ± SEM of six CSF samples analyzed in triplicate. **(B)** CSF was mixed with purified Cp and passed through a 50-kDa cutoff filter. Resulting filtrates were passed through the 3-kDa cutoff filter, and Frx activity was checked in all fractions. Unfractionated CSF and purified Cp were included for internal reference as in **(A)**. Addition of Cp doubles the Frx activity in the CSF + Cp sample, half of which is lost in the >50-kDa fraction (>50). Retentate of the 3-kDa cutoff filter (50-3 kDa) shows no activity, which is detected in the <3-kDa filtrate (<3). Data represent means ± SEM of five CSF samples analyzed in triplicate. **(C)** Purified Cp, a mix of CSF + Cp, and unfractionated CSF were treated with 50 μg/ml of PK at 37°C for 1 h. Control samples received an equivalent volume of PBS. Frx activity of purified Cp is destroyed completely by PK. The CSF + Cp samples show a significant reduction after PK, while CSF samples show no effect of PK treatment. Data represent means ± SEM of three samples analyzed in triplicate. Untreated vs. PK-treated, $*p < 0.05$, $***p < 0.001$. **(D)** As observed for the ND samples in **(A)** and **(B)** above, almost all Frx activity in DM and CJD samples is detected in the <3-kDa fraction (<3), while Cp-associated Frx activity is present in the >3-kDa fraction as expected (>3). Unfractionated CSF and Cp (whole) were analyzed in parallel for internal reference. Frx activity in the CSF of CJD cases is 2.8-fold higher than DM samples. (DM samples include two each of the randomly selected FTD, EN, and AD cases). Data are means ± SEM of six cases each of DM and CJD analyzed in triplicate. PK, proteinase-K.

associated Frx activity were processed in parallel (Fig. 5). Most of the proteins in the concentrated CSF and mouse brain homogenates fractionated in the >100- and >3-kDa fraction, respectively, where Cp and APP are expected to partition (Fig. 5A, D). Frx activity revealed a similar pattern, demonstrating Cp- and APP-specific activity (Fig. 5B, E). However, significant Frx activity was detected in the <3-kDa fraction in the CSF and brain samples despite ~10-fold less protein concentration (Fig. 5B, E). Normalization with total protein revealed maximum Frx activity in the <3-kDa fraction in both the CSF and brain samples (Fig. 5C, F). Together, these results demonstrate the presence of a nonprotein Frx in the human CSF and mouse brain homogenates.

To evaluate if Frx activity in the <3-kDa fraction arises from a small peptide, pooled CSF from the ND, DM, and sCJD cases was methanol-precipitated, and concentrated proteins were resolved by SDS-PAGE (Supplementary Fig. S3A, B), or resuspended in PBS and passed through a 3-kDa filter before evaluation. Proteins trapped in the filter were extracted by boiling in a sample buffer and analyzed in parallel (Supplementary Fig. S3A–D). Staining with silver showed a minimal difference in the protein profile of six different cases of ND, DM, and CJD before or after passing through the 3-kDa filter (Supplementary Fig. S3A–C) even after over-developing the stain (Supplementary Fig. S3C, D). No bands were visible in the <3-kDa fraction, indicating minimal protein in this fraction. However, this method does not rule out small quantities of low-molecular-weight peptides with a robust Frx activity.

The CSF Frx activity was further characterized by checking its resistance to sodium-azide and zinc, specific inhibitors of Cp and APP, respectively (22), and denaturing conditions such as boiling, prolonged incubation at room temperature, addition of Triton X-100, and repeated freeze–thawing. None of these treatments altered the Frx activity in CSF, while the activity associated with serum and purified Cp and APP decreased significantly (Fig. 6A–D, F). Moreover, Cu^{1+} was not oxidized to Cu^{2+} by the <3-kDa fraction of CSF (Fig. 6E), indicating specificity for iron (refer Supplementary Methods for details).

Discussion

We demonstrate that a combination of CSF Frx and Tf provides a disease-specific premortem diagnostic test for CJD that is superior to the currently used surrogate biomarkers.

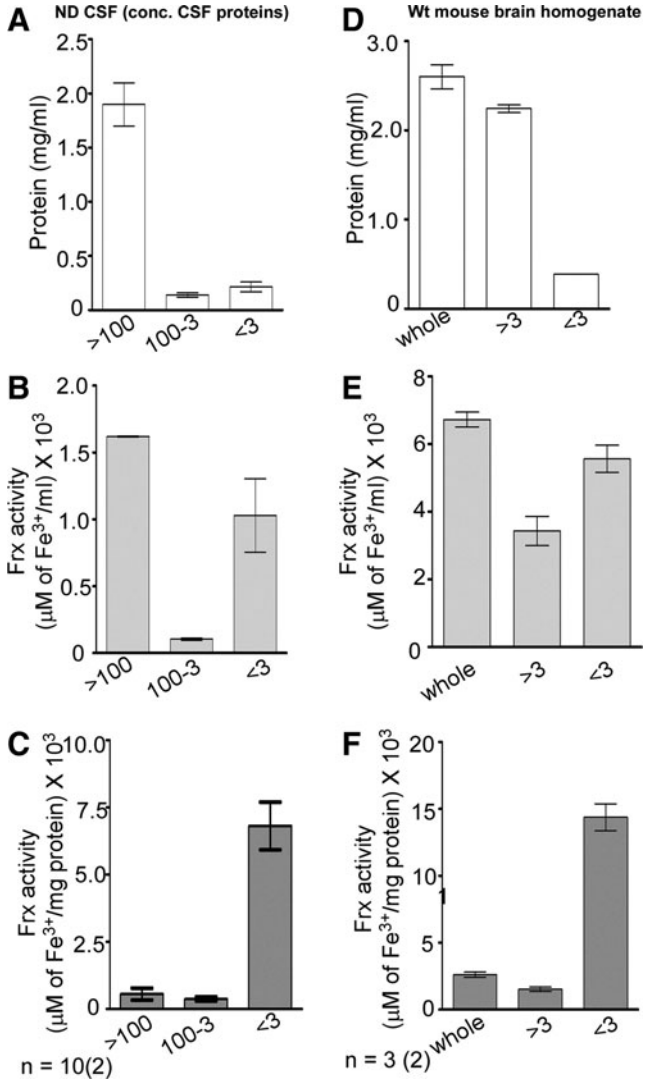

FIG. 5. Mouse brain homogenates show Frx activity in the <3-kDa fraction. (A) Proteins from pooled CSF were concentrated by methanol precipitation and fractionated sequentially through the 100- and 3-kDa filters. Majority of CSF proteins are present in the >100-kDa fraction, representing mostly Cp as expected. **(B)** Most of the Frx activity is detected in the >100-kDa fraction. However, significant Frx activity is detected in the <3-kDa fraction despite minimal protein content. **(C)** Normalization with total protein in each fraction reveals maximum Frx activity in the <3-kDa fraction. **(D)** Most of the proteins in the mouse brain homogenate fractionate in the >3-kDa fraction as expected. **(E)** Relative to the >3-kDa fraction, significantly more Frx activity is detected in the <3-kDa fraction despite 10-fold less protein content. **(F)** Normalization with total protein in each fraction reveals maximum Frx activity in the <3-kDa fraction. Data are means ± SEM of 10 pooled CSF and 3 brain samples analyzed in duplicate.

Since Frx and Tf play a vital role in brain iron metabolism, these observations indicate that the underlying cause of iron imbalance in CJD is distinct from other DMs, including AD, and is reflected in the CSF in a disease-specific manner. Unexpectedly, known brain Frxs, Cp and APP, show minimal activity in the human CSF. Instead, majority of Frx activity is nonprotein in origin, and is concentrated in the <3-kDa fraction of normal and diseased human CSF. A similar activity is detected in the normal mouse brain homogenates, revealing the presence of an uncharacterized nonprotein Frx in the brain and CSF.

Given the tight regulation of iron metabolism in the brain, it is surprising that neurodegenerative conditions of diverse etiopathogenesis and disease course such as CJD, AD, PD, and HD are associated with the brain iron imbalance (16, 37, 40, 44, 45, 69). A possible cause is the functional role of proteins implicated in the pathogenesis of these disorders in cellular iron metabolism. Thus, PrP^{C}, a substrate for the principal pathogenic agent PrP-scrapie (PrP^{Sc}) responsible for CJD, plays a functional role in cellular iron uptake and transport. A loss of function of PrP^{C} combined with sequestration of iron by the PrP^{Sc}–protein complexes is believed to induce functional iron deficiency in the CJD brains (61, 62, 63). APP and α-synuclein, proteins involved in the pathogenesis of AD and PD, possess Frx and ferrireductase activity, respectively, functions necessary for the transport and storage of cellular iron (7, 17, 22). Compromised activity of APP causes iron accumulation in the AD brains (22), though the impact of α-synuclein dysfunction on brain iron metabolism is unclear at present. Further, functional iron-responsive elements have been identified in APP and α-synuclein transcripts, suggesting their regulation by the cellular iron levels (11, 23). Huntingtin, the protein involved in the pathogenesis of HD, is also regulated by cellular iron levels (32), partially explaining the cause of iron imbalance in the HD brains. Since iron homeostasis is maintained by the coordinated regulation of several proteins, alteration of specific iron metabolic pathways due to dysfunction of these proteins is likely to influence the expression of a distinct set of proteins, and this change is likely to be reflected in the brain and CSF in a disease-specific manner.

Our results demonstrate that Frx activity is increased, and the Tf levels are decreased in premortem CSF of CJD cases relative to other-DM much before end-stage disease. In logistic regression and ROC analysis, the Frx and Tf combination performed better as a diagnostic biomarker for CJD relative to all non-CJD DMs. A sensitivity of 86.8%, specificity of 92.5%, and accuracy of 88.9% were achieved with this combination. Addition of t-tau, a biomarker currently used for the diagnosis of CJD and AD, made a minimal difference to these parameters. The Frx and Tf combination was equally effective in discriminating CJD from rapidly progressive DMs, indicating a minimal effect of neuronal death on their performance. This combination revealed a highly significant area-under-the-ROC curve of 0.94 and AIC of 0.62. A scatter plot of these biomarkers showed a minimal overlap between CJD, AD, and other-DMs, attesting to their discriminatory power. Since the accuracy of Frx and Tf in diagnosing CJD is much lower when used individually, it is likely that these proteins play a complementary role in disease processes specific to CJD. The discriminatory power of CSF Frx, but not Tf, was lost in the postmortem human and animal CSF, probably due to relative stability of the latter in biological fluids and its demonstrated utility as a diagnostic biomarker for CJD (Supplementary Fig. S4A–D) (59).

Previous reports indicate a reduction in CSF Frx activity in the AD and PD cases relative to the ND controls. The underlying cause is reduced Frx activity of Cp due to loss of

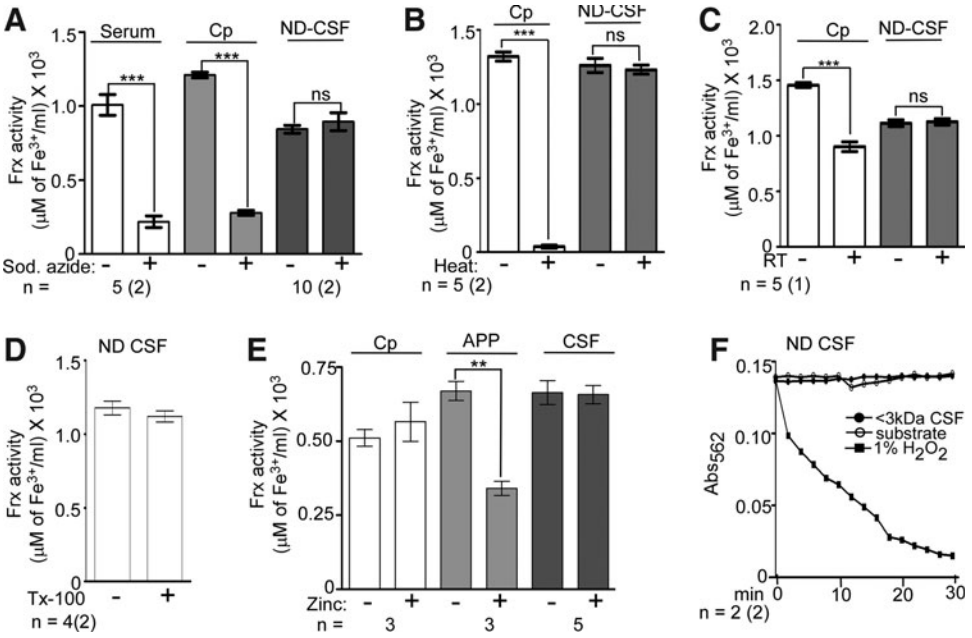

FIG. 6. Majority of Frx activity in the CSF is not from Cp. (A) Unlike serum and purified Cp, Frx activity in the <3-kDa fraction of CSF is not sensitive to sodium azide (2.5 m*M*). Data are means ± SEM of 5 serum and 10 CSF samples analyzed in duplicate; ***$p < 0.001$. **(B)** Unlike purified Cp that loses all Frx activity after heating, there is a minimal change in CSF samples. Data are means ± SEM of five CSF samples analyzed in duplicate; ***$p < 0.001$. **(C)** Unlike purified Cp, Frx activity in CSF is not reduced by repeated freeze–thawing. Data are means ± SEM of five samples analyzed in duplicate. **(D)** The CSF Frx activity is resistant to Triton X-100. Data are means ± SEM of four samples analyzed in duplicate. **(E)** Unlike purified APP, Frx activity in CSF is not sensitive to zinc (10 μM). Purified Cp is also unaffected by zinc. Data are means ± SEM of five CSF samples; **$p < 0.01$. **(F)** As opposed to H_2O_2, the <3-kDa fraction of CSF lacks copper oxidase activity. Each point represents mean ± SEM of two samples analyzed in duplicate.

copper ions or oxidation (4, 5, 9, 48). However, our results show a slight, but significant, increase in Frx activity in other DMs, including PD and AD relative to ND controls. This discrepancy is probably due to quantification of Cp-associated Frx activity in these studies (9, 48), while our assay reports the combined activity of Cp and the <3-kDa nonprotein Frx. An overall increase of Frx activity in all-DM cases relative to ND controls suggests an attempt by the iron homeostatic machinery to oxidize excess Fe^{2+} to protect against oxidative damage. However, the spectrum of Frx activity in all-DM cases overlaps to some extent with the ND and CJD cases (Fig. 1A, C). Further studies are necessary to understand the mechanism underlying the change in the CSF Frx activity in sCJD and other DMs. Disorders that are known to show significant alteration of iron-modulating proteins in the CSF include multiple sclerosis and restless-leg syndrome (13, 38, 55). Although these disorders are not associated with DM and were therefore not included in our analysis, these observations support the overall notion that the brain iron imbalance is reflected in the CSF, providing a unique opportunity to identify disease-specific biomarkers and understand disease pathogenesis.

It was surprising that neither Cp nor APP contributed significantly to the total Frx activity in the normal or diseased CSF. Although Cp and APP were detected in all CSF samples by Western blotting, only concentrated samples showed substantial Frx activity in the >100-kDa fraction. Most of the activity was in the <3-kDa fraction and resisted heat, sodium-azide, prolonged incubation at room temperature, and repeated freeze–thawing. It is likely that one or more peptides or small-molecular-weight compounds such as citrate coupled to reactive metals are responsible for this activity (39, 52). A relevant comparison is serum where although Cp is the major Frx, citrate contributes significantly to the total Frx activity (39). However, the kinetics of Frx activity associated with citrate are much slower than the activity identified in the CSF (2 h *vs.* 5 min [unpublished observations]), arguing against citrate as a possible source (39, 52). The presence of a similar Frx activity in the mouse brain homogenates suggests that nonprotein or low-molecular-weight Frxs are an important component of the brain iron homeostatic machinery, and contribute to the majority of CSF Frx activity. Based on our data, this activity does not appear to be enzymatic. Further studies are necessary to understand the nature of this Frx in detail.

In conclusion, we report the presence of the currently uncharacterized nonprotein Frx in human CSF that is increased in CJD, and, when combined with CSF Tf, provides a disease-specific premortem diagnostic test that discriminates CJD from AD, other-DMs, and rapidly progressive DMs with a superior diagnostic accuracy than that of the currently used biomarkers. Further characterization of this Frx is likely to provide information on the underlying cause of iron imbalance in CJD and other DMs, and the possibility of restoring iron homeostasis in diseased brains. Moreover, timely and accurate discrimination of treatable DMs from the currently untreatable CJD cases will allow initiation of available therapy.

Materials and Methods

Ethics statement

The use of human CSF was approved by the Case Western Reserve University (CWRU) Institutional Review Board. Personal information for all samples was limited to diagnosis, sex, and age at the time of sample collection and death. The use of mouse brain tissue was approved by the CWRU Institutional Animal Care and Use Committee (IACUC). Samples from CWD-infected deer and elk were collected and used in accordance with the guidelines reviewed and approved by the National Animal Disease Center's IACUC.

Statistical analysis

The first set of analyses compared the performance of Frx, t-tau, and t-Tf in discriminating CJD from all-DM, AD, and FTD (Table 1). *T*-tests were used to test for significant differences between disease groups. Next, the diagnostic accuracy of individual biomarkers was calculated by logistic regression. A cutoff was chosen to discriminate between positive and negative test outcomes, keeping the sensitivity of the test to ~85% following published procedures (41, 59). Specificity, positive and negative LR, PPV and NPV, and accuracy (percentage of correctly classified cases) were calculated based on the chosen cutoff. The area-under-the-ROC curve was calculated for all biomarkers. AUC has the advantage of being independent of the chosen cutoff and is therefore a reliable indicator of overall diagnostic accuracy. The ROC curve that depicts graphically the tradeoff between sensitivity and specificity for all possible cutoff values was calculated. Ninety-five percent confidence intervals (CIs) were calculated for indicators where appropriate. CIs for percentages were calculated using the efficient-score method with a continuity correction (47). CIs for LRs were calculated as proposed in a previous report (58). For AUCs, CIs were calculated, and AUCs derived from the application of different biomarkers to the same sample were compared using a nonparametric approach (18). Complete biomarker data were not available for all cases, accounting for differences in the sample number in different analyses.

Logistic regressions were tested for robustness to the introduction of subject age. Significance of the results was unaffected by this variable (Supplementary Fig. S2A, B). The influence of univariate outliers was also examined. Removal of extreme univariate outliers did not change the results significantly. The results were also tested for robustness to clustering. The data were clustered for two reasons. First, CSF samples were obtained from four different centers, creating the potential for a significant intercenter variance due to the possibility of systematic differences in sample collection and storage. Second, while Frx and Tf were measured by the authors, t-tau data for some samples were provided by the centers, creating another potential clustering effect in the t-tau data. A significant clustering effect (also known as autocorrelation) signifies that the data are not independent and identically distributed, thus violating one of the assumptions of logistic regression. When this assumption is violated, standard logistic regression analysis underestimates the standard errors of coefficients, which may lead to a statistically significant result when the result is actually nonsignificant (type I error). Consequently, intraclass correlations were calculated to determine the effect of clustering on the data. Clustering was found to have a significant effect on the t-tau and Frx values among FTD cases, when all non-CJD cases were combined. To overcome this deficiency, logistic regression analyses were repeated with a robust standard error option; the results obtained for Frx and Tf, but not t-tau, were found to be robust to clustering. Thus, while analyzing t-tau, data from centers that differed significantly were removed, leaving the cases from two centers. The analyses were repeated with this reduced sample size and found to be robust to clustering. However, the remaining number of FTD cases was too few, and analysis of CJD against FTD could not be conducted using the t-tau data.

A second set of more-stringent logistic regression analyses was used to determine the optimal combination of biomarkers for the diagnosis of sCJD. For accurate comparisons, only samples where all biomarkers were analyzed by the authors in the same laboratory were used. Cases that had limited sample volume and did not lend themselves to complete analyses were removed. This approach reduced the sample size to 144, of which 91 were sCJD and 53 DM of non-CJD origin (15 AD, 1 FTD, and 37 other-DMs). This approach removed any effect of clustering on the analyses.

Measures of diagnostic accuracy were calculated using the same procedure as above and described in a previous report (59). In addition, the AIC was calculated for each logistic regression model. AIC is useful for comparing logistic regression models, since it reflects both the model's fit to the data and its parsimony. While other indicators such as AUC increase as predictors are added to a model, the AIC indicates if the model fit improves enough to justify the loss of parsimony. Importantly, the AIC can be used to compare two models even when one is not a subset of the other. Smaller AIC values signal that a model is superior.

For the second set of analyses, multivariate outliers were identified using several different recommended techniques, and their influence on the results was assessed (42). Significance of the results was found to be robust to the removal of influential cases.

CSF samples

Premortem CSF samples from 52 cases of ND, 192 cases of DM, and 98 cases of sCJD were used for this study. All samples were snap-frozen into single-use aliquots immediately after collection and stored at −80°C until use. All samples were coded and selected randomly for each experiment. All CJD samples were collected between 2006 and 2008, DM samples between 2003 and 2011, and ND cases between January and December 2011. Detailed information of all CSF samples is provided in Supplementary Table S1.

Frx assay

Two different assays were used to quantify the Frx activity: 1) Apo-Tf assay (22), and the ammonium thiocyanate assay (4, 5). The Apo-Tf assay relies on the spectroscopic change in apo-Tf when loaded with Fe^{3+}, and was performed as described by Duce *et al.*, 2010 (22). A 200-μl reaction was set up by mixing 61 μl ddH_2O, 34 μl HBS buffer (150 m*M* NaCl and 50 m*M* HEPES, pH 7.2), 40 μl of 275 μM apo-Tf, 10 μl of CSF, and 55 μl of 400 μM FAS

$[(NH_4)_2Fe(SO_4)_2]$. BioTek Synergy 4 plate reader was preheated to 37°C, and the reaction mix was incubated at 37°C with gentle agitation for 5 min before reading the absorbance at 460 nm. The incubation time was determined after a time-course (Supplementary Fig. S1). Negative control included assay mix lacking CSF, and positive control included a measured amount of Cp. For the ammonium thiocyanate assay, 50 μl of CSF was mixed with 250 μl of 0.3 *M* acetate buffer (pH 6) and incubated at 30°C for 5 min. Subsequently, 100 μl of freshly prepared 0.01 *M* FAS solution was added and incubated for additional 5 min. The reaction was terminated by 285 μl of 1M perchloric acid, and samples were centrifuged at high speed for 3 min at 9000 *g* in an Eppendorf centrifuge. Ferric ions generated through the Frx activity of CSF were quantified in the clear supernatant by adding 685 μl of 0.5 *M* ammonium thiocyanate and measuring the change in color of the thiocyanate–Fe^{3+} complex at 450 nm in a BioTek Synergy 4 plate reader. Purified Cp (Sigma-Aldrich; Cat. No. C4519) and discarded serum from healthy donors served as positive controls. Negative controls included (i) CSF/Cp/serum incubated in an assay buffer lacking FAS to which perchloric acid was added and (ii) assay buffer without CSF/Cp/serum to which FAS and perchloric acid were added. The amount of purified Cp and serum was titrated to obtain the equivalent activity relative to CSF. Copper-oxidase activity was determined as described (20).

Please see Supplementary Materials for complete methods.

Acknowledgments

We thank Pierluigi Gambetti, the Director of the National Prion Disease Pathology Surveillance Center (NPDPSC), for providing CSF samples of the sCJD and DM cases. This study was funded by NIH grants NS077438, NS076139, and DK088390 to N.S.

Author Contributions

S.H. performed all experiments, wrote first draft, edited manuscript. A.J.B. performed statistical analyses and wrote the section. N.S. conceived the idea, wrote the manuscript, overlooked experimental work. J.W. and A.S. helped in experimental work. Other authors provided CSF samples and intellectual input.

Author Disclosure Statement

All authors declare that no competing financial interests exist.

References

1. Aguzzi A and Falsig J. Prion propagation, toxicity and degradation. *Nat Neurosci* 15: 936–939, 2012.
2. Atarashi R, Satoh K, Sano K, Fuse T, Yamaguchi N, Ishibashi D, Matsubara T, Nakagaki T, Yamanaka H, Shirabe S, Yamada M, Mizusawa H, Kitamoto T, Klug G, McGlade A, Collins SJ, and Nishida N. Ultrasensitive human prion detection in cerebrospinal fluid by real-time quaking-induced conversion. *Nat Med* 17: 175–178, 2011.
3. Barone E, Di Domenico F, Sultana R, Coccia R, Mancuso C, Perluigi M, and Butterfield DA. Heme oxygenase-1 post-translational modifications in the brain of subjects with Alzheimer disease and mild cognitive impairment. *Free Radic Biol Med* 52: 2292–2301, 2012.
4. Boll MC, Alcaraz-Zubeldia M, Montes S, and Rios C. Free copper, ferroxidase and SOD1 activities, lipid peroxidation and NO(x) content in the CSF. A different marker profile in four neurodegenerative diseases. *Neurochem Res* 33: 1717–1723, 2008.
5. Boll MC, Sotelo J, Otero E, Alcaraz-Zubeldia M, and Rios C. Reduced ferroxidase activity in the cerebrospinal fluid from patients with Parkinson's disease. *Neurosci Lett* 265: 155–158, 1999.
6. Bonda DJ, Lee HG, Blair JA, Zhu X, Perry G, and Smith MA. Role of metal dyshomeostasis in Alzheimer's disease. *Metallomics* 3: 267–270, 2011.
7. Cahill CM, Lahiri DK, Huang X, and Rogers JT. Amyloid precursor protein and alpha synuclein translation, implications for iron and inflammation in neurodegenerative disease. *Biochim Biophys Acta* 1790: 615–628, 2009.
8. Calabrese V, Sultana R, Scapagnini G, Guagliano E, Sapienza M, Bella R, Kanski J, Pennisi G, Mancuso C, Stella AM, and Butterfield DA. Nitrosative stress, cellular stress response, and thiol homeostasis in patients with Alzheimer's disease. *Antioxid Redox Signal* 8: 1975–1986, 2006.
9. Capo CR, Arciello M, Squitti R, Cassetta E, Rossini PM, Calabrese L, and Rossi L. Features of ceruloplasmin in the cerebrospinal fluid of Alzheimer's disease patients. *Biometals* 21: 367–372, 2008.
10. Chitravas N, Jung RS, Kofskey DM, Blevins JE, Gambetti P, Leigh RJ, and Cohen ML. Treatable neurological disorders misdiagnosed as Creutzfeldt-Jakob disease. *Ann Neurol* 70: 437–444, 2011.
11. Cho HH, Cahill CM, Vanderburg CR, Scherzer CR, Wang B, Huang X, and Rogers JT. Selective translational control of the Alzheimer amyloid precursor protein transcript by iron regulatory protein-1. *J Biol Chem* 285: 31217–31232, 2010.
12. Chohan G, Pennington C, Mackenzie JM, Andrews M, Everington D, Will RG, Knight RS, and Green AJ. The role of cerebrospinal fluid 14-3-3 and other proteins in the diagnosis of sporadic Creutzfeldt-Jakob disease in the UK: a 10-year review. *J Neurol Neurosurg Psychiatry* 81: 1243–1248, 2010.
13. Clardy SL, Earley CJ, Allen RP, Beard JL, and Connor JR. Ferritin subunits in CSF are decreased in restless legs syndrome. *J Lab Clin Med* 147: 67–73, 2006.
14. Cosseddu GM, Nonno R, Vaccari G, Bucalossi C, Fernandez-Borges N, Di Bari MA, Castilla J, and Agrimi U. Ultra-efficient PrP(Sc) amplification highlights potentialities and pitfalls of PMCA technology. *PLoS Pathog* 7: e1002370, 2011.
15. Coulthart MB, Jansen GH, Olsen E, Godal DL, Connolly T, Choi BC, Wang Z, and Cashman NR. Diagnostic accuracy of cerebrospinal fluid protein markers for sporadic Creutzfeldt-Jakob disease in Canada: a 6-year prospective study. *BMC Neurol* 11: 133, 2011.
16. Crichton RR, Dexter DT, and Ward RJ. Brain iron metabolism and its perturbation in neurological diseases. *J Neural Transm* 118: 301–314, 2011.
17. Davies P, Moualla D, and Brown DR. Alpha-synuclein is a cellular ferrireductase. *PLoS One* 6: e15814, 2011.
18. DeLong ER, DeLong DM, and Clarke-Pearson DL. Comparing the areas under two or more correlated receiver operating characteristic curves: a nonparametric approach. *Biometrics* 44: 837–845, 1998.
19. Di Domenico F, Barone E, Mancuso C, Perluigi M, Cocciolo A, Mecocci P, Butterfield DA, and Coccia R. HO-1/BVR-A

system analysis in plasma from probable Alzheimer's disease and mild cognitive impairment subjects: a potential biochemical marker for the prediction of the disease. *J Alzheimers Dis* 32: 277–289, 2012.
20. Djoko KY, Chong LX, Wedd AG, and Xiao Z. Reaction mechanisms of the multicopper oxidase CueO from *Escherichia coli* support its functional role as a cuprous oxidase. *J Am Chem Soc* 132: 2005–2015, 2010.
21. Doran M and Larner AJ. EEG findings in dementia with Lewy bodies causing diagnostic confusion with sporadic Creutzfeldt-Jakob disease. *Eur J Neurol* 11: 838–841, 2004.
22. Duce JA, Tsatsanis A, Cater MA, James SA, Robb E, Wikhe K, Leong SL, Perez K, Johanssen T, Greenough MA, Cho HH, Galatis D, Moir RD, Masters CL, McLean C, Tanzi RE, Cappai R, Barnham KJ, Ciccotosto GD, Rogers JT, and Bush AI. Iron-export ferroxidase activity of β-amyloid precursor protein is inhibited by zinc in Alzheimer's Disease. *Cell* 142: 857–867, 2010.
23. Friedlich AL, Tanzi RE, and Rogers JT. (2007) The 5′-untranslated region of Parkinson's disease alpha-synuclein messenger RNA contains a predicted iron responsive element. *Mol Psychiatry* 12: 222–223, 2007.
24. Gaig C, Valldeoriola F, Gelpi E, Ezquerra M, Llufriu S, Buongiorno M, Jesús Rey M, Jose Martí M, Graus F, and Tolosa E. Rapidly progressive diffuse Lewy body disease. *Mov Disord* 26: 1316–1323, 2011.
25. Geschwind MD, Haman A, and Miller BL. Rapidly progressive dementia. *Neurol Clin* 25: 783–807, 2007.
26. Geschwind MD, Martindale J, Miller D, DeArmond SJ, Uyehara-Lock J, Gaskin D, Kramer JH, Barbaro NM, and Miller BL. Challenging the clinical utility of the 14-3-3 protein for the diagnosis of sporadic Creutzfeldt-Jakob disease. *Arch Neurol* 60: 813–816, 2003.
27. Geschwind MD, Shu H, Haman A, Sejvar JJ, and Miller BL. Rapidly progressive dementia. *Ann Neurol* 64: 97–108, 2008.
28. Gray LW, Kidane TZ, Nguyen A, Akagi S, Petrasek K, Chu YL, Cabrera A, Kantardjieff K, Mason AZ, and Linder MC. Copper proteins and ferroxidases in human plasma and that of wild-type and ceruloplasmin knockout mice. *Biochem J* 419: 237–245, 2009.
29. Haïk S, Brandel JP, Sazdovitch V, Delasnerie-Lauprêtre N, Peoc'h K, Laplanche J-L, Privat N, Duyckaerts C, Kemeny JL, Kopp N, Laquerrière A, Mohr M, Deslys JP, Dormont D, and Hauw JJ. Dementia with Lewy bodies in a neuropathologic series of suspected Creutzfeldt-Jakob disease. *Neurology* 55: 1401–1404, 2000.
30. Hamlin C, Puoti G, Berri S, Sting E, Harris C, Cohen M, Spear C, Bizzi A, Debanne SM, and Rowland DY. A comparison of tau and 14-3-3 protein in the diagnosis of Creutzfeldt-Jakob disease. *Neurology* 79: 547–552, 2012.
31. Heinemann U, Krasnianski A, Meissner B, Varges D, Kallenberg K, Schulz-Schaeffer WJ, Steinhoff BJ, Grasbon-Frodl EM, Kretzschmar HA, and Zerr I. Creutzfeldt-Jakob disease in Germany: a prospective 12-year surveillance. *Brain* 130: 1350–1359, 2007.
32. Hilditch-Maguire P, Trettel F, Passani LA, Auerbach A, Persichetti F, and MacDonald ME. (2000) Huntingtin: an iron regulated protein essential for normal nuclear and perinuclear organelles. *Hum Mol Genet* 9: 2789–2797, 2000.
33. Holtzman DM. CSF biomarkers for Alzheimer's disease: current utility and potential future use. *Neurobiology* 32: S4–S9, 2011.
34. Hwang D, Lee IY, Yoo H, Gehlenborg N, Cho JH, Petritis B, Baxter D, Pitstick R, Young R, Spicer D, Price ND, Hohmann JG, Dearmond SJ, Carlson GA, and Hood LE. A systems approach to prion disease. *Mol Syst Biol* 5: 252, 2009.
35. Jayaratnam S, Khoo AK, and Basic D. Rapidly progressive Alzheimer's disease and elevated 14-3-3 proteins in cerebrospinal fluid. *Age Ageing* 37: 467–469, 2008.
36. Jeong SY and David S. Glycosylphosphatidylinositol-anchored ceruloplasmin is required for iron efflux from cells in the central nervous system. *J Biol Chem* 278: 27144–27148, 2003.
37. Kell DB. Towards a unifying, systems biology understanding of large-scale cellular death and destruction caused by poorly liganded iron: Parkinson's, Huntington's, Alzheimer's, prions, bactericides, chemical toxicology and others as examples. *Arch Toxicol* 84: 825–889, 2010.
38. Khalil M, Teunissen C, and Langkammer C. Iron and neurodegeneration in multiple sclerosis. *Mult Scler Int* 2011: 606807, 2011.
39. Lee GR, Nacht S, Christensen D, Hansen SP, and Cartwright GE. The contribution of citrate to the ferroxidase activity of serum. *Exp Biol Med* 131: 918–923, 1969.
40. MacKenzie EL, Iwasaki K, and Tsuji Y. Intracellular iron transport and storage: from molecular mechanisms to health implications. *Antioxid Redox Signal* 10: 997–1030, 2001.
41. Mattsson N, Zetterberg H, Hansson O, Andreasen N, Parnetti L, Jonsson M, Herukka SK, van der Flier WM, Blankenstein MA, Ewers M, Rich K, Kaiser E, Verbeek M, Tsolaki M, Mulugeta E, Rosén E, Aarsland D, Visser PJ, Schröder J, Marcusson J, de Leon M, Hampel H, Scheltens P, Pirttilä T, Wallin A, Jönhagen ME, Minthon L, Winblad B, and Blennow K. CSF Biomarkers and incipient Alzheimer disease in patients with mild cognitive impairment. *JAMA* 302: 385–393, 2009.
42. Menard S. *Applied Logistic Regression Analysis. Sage University Paper Series on Quantitative Applications in the Social Sciences, 07-106*. Thousand Oaks, CA: Sage, 1995.
43. Meyne F, Gloeckner SF, Ciesielczyk B, Heinemann U, Krasnianski A, Meissner B, and Zerr I. Total prion protein levels in the cerebrospinal fluid are reduced in patients with various neurological disorders. *J Alzheimers Dis* 17: 863–873, 2009.
44. Moos T and Morgan EH. The metabolism of neuronal iron and its pathogenic role in neurological disease: review. *Ann N Y Acad Sci* 1012: 14–26, 2004.
45. Moos T, Rosengren Nielsen T, Skjørringe T, and Morgan EH. Iron trafficking inside the brain. *J Neurochem* 103: 1730–1740, 2007.
46. Muayqil T, Gronseth G, and Camicioli R. Evidence-based guideline: Diagnostic accuracy of CSF 14-3-3 protein in sporadic Creutzfeldt-Jakob disease: Report of the Guideline Development Subcommittee of the American Academy of Neurology. *Neurology* 79: 1499–1506, 2012.
47. Newcombe RG. Two-sided confidence intervals for the single proportion: Comparison of seven methods. *Stat Med* 17: 857–872, 1998.
48. Olivieri S, Conti A, Iannaccone S, Cannistraci CV, Campanella A, Barbariga M, Codazzi F, Pelizzoni I, Magnani G, Pesca M, Franciotta D, Cappa SF, and Alessio M. Ceruloplasmin oxidation, a feature of Parkinson's disease CSF, inhibits ferroxidase activity and promotes cellular iron retention. *J Neurosci* 31: 18568–18577, 2011.
49. Orrú CD, Wilham JM, Hughson AG, Raymond LD, McNally KL, Bossers A, Ligios C, and Caughey B. Human variant Creutzfeldt-Jakob disease and sheep scrapie PrP(res) detection using seeded conversion of recombinant prion protein. *Protein Eng Des Sel* 22: 515–521, 2009.
50. Pennington C, Chohan G, Mackenzie J, Andrews M, Will R, Knight R, and Green A. The role of cerebrospinal fluid

proteins as early diagnostic markers for sporadic Creutzfeldt-Jakob disease. *Neurosci Lett* 455: 56–59, 2009.
51. Perry DC and Geschwind MD. Thorough work-up and new diagnostic criteria needed for CJD. *Nat Rev Neurol* 7: 479–480, 2011.
52. Pham AN and Waite TD. Modeling the kinetics of Fe(II) oxidation in the presence of citrate and salicylate in aqueous solutions at pH 6.0–8.0 and 25 30)degrees C. *J Phys Chem A* 112: 5395–5405, 2008.
53. Puoti G, Bizzi A, Forloni G, Safar JG, Tagliavini F, and Gambetti P. Sporadic human prion diseases: molecular insights and diagnosis. *Lancet Neurol* 11: 618–628, 2012.
54. Schmidt C, Wolff M, Weitz M, Bartlau T, Korth C, and Zerr I. Rapidly progressive Alzheimer disease. *Arch Neurol* 68: 1124–1130, 2011.
55. Sfagos C, Makis AC, Chaidos A, Hatzimichael EC, Dalamaga A, Kosma K, and Bourantas KL. Serum ferritin, transferrin and soluble transferrin receptor levels in multiple sclerosis patients. *Mult Scler* 11: 272–275, 2005.
56. Shaw LM, Korecka M, Clark CM, Lee VM, and Trojanowski JQ. Biomarkers of neurodegeneration for diagnosis and monitoring therapeutics. *Nat Rev Drug Discov* 6: 295–303, 2007.
57. Siman R, Giovannone N, Toraskar N, Frangos S, Stein SC, Levine JM, and Kumar MA. Evidence that a panel of neurodegeneration biomarkers predicts vasospasm, infarction, and outcome in aneurysmal subarachnoid hemorrhage. *PLoS One* 6: e28938, 2011.
58. Simel DL, Samsa GP, and Matchar DB. Likelihood ratios with confidence: sample size estimation for diagnostic test studies. *J Clin Epidemiol* 44: 763–770, 1991.
59. Singh A, Beveridge AJ, and Singh N. Decreased CSF Transferrin in sCJD: A Potential Pre-Mortem Diagnostic Test for Prion Disorders. *PLoS One* 6: e16804, 2011.
60. Singh A, Isaac AO, Luo X, Mohan, ML, Bartz J, and Singh N. Abnormal brain iron homeostasis in human and animal prion disorders. *PLoS Pathog* 5: e1000336, 2009.
61. Singh A, Kong Q, Luo X, Petersen RB, Meyerson H, and Singh N. Prion protein (PrP) knock-out mice show altered iron metabolism: a functional role for PrP in iron uptake and transport. *PLoS One* 4: e6115, 2009.
62. Singh A, Mohan ML, Isaac AO, Luo X, Petrak J, Vyoral D, and Singh N. Prion protein modulates cellular iron uptake: a novel function with implications for disease pathogenesis. *PLoS One* 4: e4468, 2009.
63. Singh A, Qing L, Kong Q, and Singh N (2012) Change in the characteristics of ferritin induces iron imbalance in prion disease affected brains. *Neurobiol Dis* 45: 930–938, 2012.
64. Singh N, Das D, Singh A, and Mohan ML. Prion protein and metal interaction: physiological and pathological implications. *Curr Issues Mol Biol* 12: 99–107, 2010.
65. Singh N, Singh A, Das D, and Mohan ML. Redox control of prion and disease pathogenesis. *Antioxid Redox Signal* 12: 1271–1294, 2010.
66. This reference has been deleted.
67. Taipa R, Pinho J, and Melo-Pires M. Clinico-pathological correlations of the most common neurodegenerative dementias. *Front Neurol* 3: 68, 2012.
68. Tartaglia MC, Johnson DY, Thai JN, Cattaruzza T, Wong K, Garcia P, Dearmond SJ, Miller BL, and Geschwind MD. Clinical overlap between Jakob-Creutzfeldt disease and Lewy body disease. *Can J Neurol Sci* 39: 304–310, 2012.
69. Thompson KJ, Shoham S, and Connor JR. Iron and neurodegenerative disorders. *Brain Res Bull* 55: 155–164, 2001.
70. Torres M, Cartier L, Matamala JM, Hernández N, Woehlbier U, and Hetz C. Altered Prion protein expression pattern in CSF as a biomarker for Creutzfeldt-Jakob disease. *PLoS One* 7: e36159, 2012.
71. Tschampa HJ, Neumann M, Zerr I, Henkel K, Schröter A, Schulz-Schaeffer WJ, Steinhoff BJ, Kretzschmar HA, and Poser S. Patients with Alzheimer's disease and dementia with Lewy bodies mistaken for Creutzfeldt-Jakob disease. *J Neurol Neurosurg Psychiatry* 71: 33–39, 2001.
72. Watts JC, Balachandran A, and Westaway D. The expanding universe of prion diseases. *PLoS Pathog* 2: e26, 2006.
73. Wolozin B and Golts N. Iron and Parkinson's disease. *Neuroscientist* 8: 22–32, 2002.
74. World Health Organization. Consensus on criteria for sporadic CJD. *Wkly Epidemiol Rec* 73: 361–365, 1998.
75. Zerr I, Kallenberg K, Summers DM, Romero C, Taratuto A, Heinemann U, Breithaupt M, Varges D, Meissner B, Ladogana A, Schuur M, Haik S, Collins SJ, Jansen GH, Stokin GB, Pimentel J, Hewer E, Collie D, Smith P, Roberts H, Brandel JP, van Duijn C, Pocchiari M, Begue C, Cras P, Will RG, and Sanchez-Juan P. Updated clinical diagnostic criteria for sporadic Creutzfeldt-Jakob disease. *Brain* 132: 2659–2668, 2009.

Address correspondence to:
Dr. Neena Singh
Department of Pathology
Case Western Reserve University
2103 Cornell Road
Cleveland, OH 44106

E-mail: neena.singh@case.edu

Date of first submission to ARS Central, October 23, 2012; date of final revised submission, February 1, 2013; date of acceptance, February 4, 2013.

Abbreviations Used

AD = Alzheimer's disease
AIC = Aikake-Information Criterion
APP = amyloid precursor protein
AUC = area under the curve
CI = confidence interval
Cp = ceruloplasmin
CSF = cerebrospinal fluid
CWRU = Case Western Reserve University
DM = dementia
EN = encephalitis
FAS = ferrous ammonium sulfate
Frx = ferroxidase
FTD = frontotemporal dementia
HD = Huntington's disease
LR = likelihood ratios
ND = nondementia
NPV = negative predictive value
NSE = neuron-specific enolase
PD = Parkinson's disease
PK = proteinase-K
PPV = positive predictive value
ROC = receiver-operating characteristic
sCJD = sporadic Creutzfeldt-Jakob disease
Tf = transferrin
VS = progressive cerebral vasculitis
WHO = World Health Organization